International Journal of Pharmaceutics 385 (2010) 143–149

Contents lists available at ScienceDirect

International Journal of Pharmaceutics

journal homepage: www.elsevier.com/locate/ijpharm

Pharmaceutical Nanotechnology

Gelatin nanocarriers as potential vectors for effective management of tuberculosis

Gaurav Kant Saraogi [a], Puspa Gupta [b], U.D. Gupta [b], N.K. Jain [a], G.P. Agrawal [a,*]

[a] Pharmaceutics Research Laboratory, Department of Pharmaceutical Sciences, Dr. H.S. Gour University, Sagar, MP 470003, India
[b] National JALMA Institute for Leprosy and Other Mycobacterial Diseases (ICMR), Agra, UP 282001, India

ARTICLE INFO

Article history:
Received 1 July 2009
Received in revised form
26 September 2009
Accepted 1 October 2009
Available online 9 October 2009

Keywords:
Rifampicin
Tuberculosis
Drug delivery
Nanoparticles
Gelatin nanoparticles

ABSTRACT

The aim of the research work was to develop and characterize rifampicin (RIF) loaded gelatin nanoparticulate delivery system for the effective management of tuberculosis. Gelatin nanoparticles (GPs) containing RIF were prepared using two-step desolvation method. Formulations were characterized through transmission electron microscopy (TEM), atomic force microscopy (AFM), size and size distribution analysis, polydispersity index (PDI), zeta potential, percent drug entrapment, percent nanoparticulate yield and *in vitro* drug release. Formulations were further characterized for *in vitro* cytotoxicity, *in vivo* biodistribution, and antitubercular activity. The nanoparticles were found to be spherical in shape. The size of nanoparticles was found to be 264 ± 11.2 nm with low PDI suggesting the narrow particle size distribution. The drug release showed the biphasic pattern of release i.e. initial burst followed by a sustained release pattern. The cytotoxicity studies revealed that nanoparticles are safe, non toxic as compared to free drug. *In vivo* biodistribution study showed higher localization of RIF loaded GPs in various organs, as compared to plain RIF solution in PBS (pH 7.4). In contrast to free drug, the nanoparticles not only sustained the plasma level but also enhanced the AUC and mean residence time (MRT) of the drug, suggesting improved pharmacokinetics of drug. RIF GPs additionally resulted in significant reduction in bacterial counts in the lungs and spleen of TB-infected mice. Hence, GPs hold promising potential for increasing drug targetability *vis a vis* reducing dosing frequency with the interception of minimal side effects, for efficient management of tuberculosis.

1. Introduction

Tuberculosis (TB) is the leading infectious killer of youth and adults worldwide due to a single infectious agent and the second most common cause of death amongst infectious diseases, after acquired immunodeficiency syndrome (AIDS). Approximately one-third of the world population—i.e. two billion people are, infected with *Mycobacterium tuberculosis* (*M. tuberculosis*), more than eight million people develop TB every year, and approximately two million die annually (World Health Organization, 2006; Gupta and Katoch, 2009). Although effective drugs are available for treatment of TB, yet daily multiple drug therapy for several months, poor patient compliance, drug toxicity and emergence of multi drug resistance lead to failure of chemotherapy (Toit et al., 2006). Rifampicin (RIF) is first line drug currently used for treatment of latent *M. tuberculosis* infection in adults. But a number of side effects like lack of appetite, nausea, hepatotoxicity, fever, chill, allergic rashes, itching and immunological disturbances, patient non-compliance in long term therapy limit its use (Barrow et al., 1998; Laura et al., 2000). Thus, the current strategy for enhancing the therapeutic activity of currently available drugs is to entrap drugs within a delivery system from where they are slowly released over an extended time period (Gelperina et al., 2005). Novel drug carrier systems play an important role in controlled delivery of a pharmaceutical agent to the target at therapeutically optimal rate and dose. Several reports are available regarding the use of carrier systems like liposomes, dendrimers, microspheres, solid lipid nanoparticles for delivery of bioactives. Amongst various drug delivery systems, nanoparticles (NPs) represent a very promising approach for deliver bioactives (Deol and Khuller, 1997; Kreuter, 2004; Pandey and Khuller, 2005; Kumar et al., 2006).

Nanoparticles represent a class of drug delivery vehicles which can serve as promising perspective for ferrying large doses of the drug to the target site with interception of minimal side effects. As a drug delivery carrier they offer several advantages, such as ease of purification and sterilization, possibility of drug targeting, and a sustained release action (Soppimath et al., 2001; Gelperina et al., 2005; Kisich et al., 2007; Pandey and Khuller, 2007; Ahmad et al., 2008). Targeted drug delivery systems can optimize the therapeutic index of antitubercular drugs by increasing the drug concentra-

* Corresponding author. Tel.: +91 9424450204.
E-mail address: gpagrawal2005@rediffmail.com (G.P. Agrawal).

0378-5173/$ – see front matter © 2009 Elsevier B.V. All rights reserved.
doi:10.1016/j.ijpharm.2009.10.004

tion ratio of diseased tissue to normal tissue (Sharma et al., 2004). Compared to other carrier systems, nanoparticles are known to have better accumulation in macrophage rich organs, e.g., lungs, liver, and spleen because of their preferential phagocytosis (Bala et al., 2004). It is well known that pulmonary TB is the commonest form of TB and alveolar macrophages of lungs being the abode of *M. tuberculosis*. Therefore, nanoparticles represent an interesting carrier system for the delivery of antitubercular agents to the macrophages as an attempt to reduce the required dose, to minimize toxicity, to minimize dose dependent side effects, to sustain the drug release, and selectively deliver the drug to infected cells (Gelperina et al., 2005).

Nanoparticles synthesized from various biodegradable polymers like alginate, poly(lactide-co-glycolide), chitosan with antitubercular drugs have been investigated. Gelatin nanoparticles (GPs) offer a number of benefits because of their biocompatibility, biodegradability, low antigenicity, low cost, numerous available active groups for attaching targeting molecules and ease of their use as parenteral formulations (Coester et al., 2000; Verma et al., 2005; Kaur et al., 2008). GPs have been previously reported for the delivery of bioactives like amphotericin B, paclitaxel, methotrexate, doxorubicin, chloroquine phosphate and also for gene delivery and peptide drugs (Nahar et al., 2008; Leo et al., 1997; Li et al., 1998; Truong-Le et al., 1999; Cascone et al., 2002; Kaul and Amiji, 2005; Yeh et al., 2005; Bajpai and Choubey, 2006) and also for cancer therapy as antibody anchored GPs for targeting leukemic cells and primary T lymphocytes (Balthasar et al., 2005). Various methods, like emulsification-solvent evaporation, desolvation, and coacervation-phase separation, have been employed to prepare GPs (Li et al., 1998; Cascone et al., 2002; Bajpai and Choubey, 2006). In order to obtain nanoparticles of uniform shape, desolvation method is more appropriate. A desolvating agent (e.g. a salt solution, alcohol and acetone) is added to an aqueous gelatin solution in order to dehydrate the gelatin molecules, resulting in a change in conformation from stretched to coiled structure, indicated by a rise in turbidity. Next, a cross-linking agent is added to harden the native particles (Coester et al., 2000; Nahar et al., 2008; Verma et al., 2005). GPs prepared by these methods were found to be large in size, having irreversible aggregation tendency, lower stability and a high PDI due to heterogeneity in molecular weight of the gelatin polymer, which may affect the drug release, drug loading, etc.

In the present study, RIF-loaded GPs were fabricated with the use of two-step desolvation method using acetone as desolvating agent and the GPs were characterized by various physicochemical means such as size measurements, drug entrapment and *in vitro* drug release. The formulations were further evaluated for cytotoxicity study on J-774 macrophage cell lines and *in vivo* biodistribution and antitubercular studies were performed on mice model.

2. Material and methods

2.1. Materials

Rifampicin (RIF) was obtained as a benevolent gift sample from Lupin Pvt. Ltd., India. Gelatin type A (Bloom 175), MTT (3-(4,5-dimethylthiazol-2-yl)-2,5-diphenyltetrazolium bromide) dye were procured from Sigma, USA. RPMI-1640, fetal calf serum (FCS), penicillin, streptomycin, sodium pyruvate were procured from Genetix Biotech Asia Pvt. Ltd., India. Gluteraldehyde, acetone and methanol, dimethyl sulphoxide were purchased from Central Drug House Ltd., India. *M. tuberculosis* H37Rv was kindly provided by Dr. J.S. Tyagi, All India institute of medical sciences, New Delhi, India. All other chemicals were of analytical grade and used as received without any further modification.

2.2. Preparation of GPs

Nanoparticles were prepared using the double desolvation method described by Coester et al. (2000) with slight modifications. Briefly 2% (w/v) of gelatin was dissolved in water (10 mL) by maintaining temperature at $40 \pm 1\,^{\circ}C$. Acetone was added to the gelatin solution (10 mL) as a desolvating agent to precipitate the high molecular mass (HMM) gelatin. The supernatant was discarded and the HMM gelatin was redissolved in 10 mL distilled water under constant stirring at 1200 rpm (Remi, Mumbai, India). The pH of the solution was adjusted to 3.0. The gelatin was then desolvated again by drop wise addition of acetone under constant stirring (1200 rpm) for 30 min. The formed gelatin nanoparticles were cross linked with 200 μL aqueous gluteraldehyde solution (25%, v/v) at room temperature and the solution was stirred for 12 h at 1200 rpm. The excess of glutaraldehyde was neutralized using cysteine and nanoparticles prepared were then sonicated for 2 min (Jain et al., 2008). The particles were then purified by centrifugation at $10{,}000 \times g$ for 20 min and the resulting nanoparticles were stored in refrigeration. The drug (0.1%, w/w) solution was added just before the second desolvation step.

2.3. Characterization of nanoparticles

2.3.1. Shape

The morphology of GPs was determined by transmission electron microscopy using Philips EM268D instrument (Philips, The Netherlands). The aqueous dispersion (one drop) was placed over a 400-mesh carbon-coated copper grid followed by negative staining with phosphotungstic acid solution (3%, w/v, adjusted to pH 4.7 with KOH) and placed at the accelerating voltage of 95 kV. Atomic force microscopy (AFM) of GPs was taken using a Digital Nanoscope IV Bioscope (Veeco Instruments, Santa Barbara, CA, USA). Samples were prepared by spreading a drop of nanoparticles solution on a degreased glass plate uniformly.

2.3.2. Size and zeta potential

The particle size and size distribution of the nanoparticle was determined by the laser diffraction method (Nano Z.S., Malvern Instruments Inc., Worcestershire, UK). The nanoparticle suspension (1.0 mL) was dispersed in 4.0 mL deionized water. Measurements were carried out at $25 \pm 1\,^{\circ}C$ by scattering the light at 90°. The mean particle size and size distribution were determined. The zeta potential of the formulations was determined by laser doppler anemometry using a Zetasizer (Malvern Instruments, Worcestershire, UK). For the measurement, 100 μL of nanoparticle suspension was diluted to 4 mL with 10 mM NaCl solution followed by adjustment of pH to 8.0, using 0.25N HCl or NaOH. An electric field of 150 mV was applied to measure the electrophoretic velocity of the particles. All the measurements were made at room temperature, in triplicate.

2.3.3. Entrapment efficiency

Entrapment efficiency of nanoparticles was determined by the method proposed by Vandervoort and Ludwig (2004). The amount of RIF entrapped was determined by incubating the nanoparticle suspension (1.0 mL) in 5.0 mL phosphate buffer saline (PBS, pH 7.4) for 2 h at 800 rpm at $25 \pm 1\,^{\circ}C$ on a magnetic stirrer (Remi, Mumbai, India). The amount of unentrapped drug was determined spectrophotometrically (Shimadzu, 1601; Kyoto, Japan) in the supernatant obtained after separation of nanoparticles by centrifugation at $10{,}000 \times g$ for 30 min by using Eq. (1):

$$\text{Drug entrapment}\,(\%) = \frac{\text{Amount of drug used in formulation} - \text{amount of unbound drug}}{\text{Amount of drug used in formulation}} \times 100 \quad (1)$$

The purified nanoparticulate suspension was ultracentrifuged (L-8 60M; Beckman, Buckinghamshire, UK) at 30,000 × *g* for 1 h at 4 ± 1 °C. The supernatant was discarded and the pellet was freeze-dried. The yields of various GPs were calculated using Eq. (2):

$$\text{Nanoparticles yield (w/w\%)} = \frac{\text{Amount of recovered GPs}}{\text{Total amount of polymer and drug added}} \times 100 \quad (2)$$

The actual drug contents of GPs were calculated after digesting nanoparticles enzymatically using trypsin (200 μg/mL) at a trypsin-to-nanoparticles ratio of 1:5 (w/w) and mixture was kept under magnetic stirring for 5 h and clear solution was obtained, and free drug was estimated spectrophotometrically (Nahar et al., 2008). Actual dug content was calculated by using Eq. (3):

$$\text{Actual drug loading (w/w\%)} = \frac{\text{Amount of drug in GPs}}{\text{Amount of GPs recovered}} \times 100 \quad (3)$$

2.3.4. UV–vis spectroscopy

UV–vis spectra of pure RIF as well as RIF-loaded GPs were obtained using UV–vis spectrophotometer (Shimadzu1601; Kyoto, Japan). Briefly, RIF-loaded GPs were dispersed in 5.0 mL of phosphate buffer saline (PBS, pH 7.4) to give a final RIF concentration of 10 μg/mL. The suspension was then filtered through a 0.45-μm membrane filter and scanned in the range of 200–600 nm against plain nanoparticles as blank (Gallo and Radaelli, 2005).

2.3.5. In vitro drug release

Drug release from known amounts of RIF loaded GPs nanoparticles was evaluated using the equilibrium dialysis technique at 37 ± 1 °C and quantification was carried out by spectrophotometric method (Leo et al., 1997). Briefly, 2 mL of nanoparticle dispersion was put in the dialysis bag (MWCO 12,000–14,000 Da, Himedia, India) and were dialyzed against 50 mL of PBS (pH 7.4) with 200 mg/mL ascorbic acid, which was added as an antioxidant to prevent oxidative degradation of RIF at a rotation speed of 50 rpm (Kumar et al., 2006). At predetermined time intervals, 0.5 mL samples were withdrawn through sampling port, filtered through 0.45 μm membrane filter and the drug content was determined spectrophotometrically. The receptor phase volume was replenished with an equal volume of fresh PBS maintained at 37 ± 1 °C. Each diffusion experiment was performed three times, and the mean values and standard deviations were calculated.

2.3.6. Ex vivo cytotoxicity study (MTT assay)

The MTT (3-(4,5-dimethylthiazol-2-yl)-2,5-diphenyltetrazolium bromide) assay is a simple non-radioactive colorimetric assay to measure cell cytotoxicity, cell proliferation or viability. To determine cytotoxicity/viability, the J-774 macrophage cells were plated at a cell density of 1.5×10^5 cells per well in 96-well plates and incubated at 37 ± 1 °C in an atmosphere of 5% CO_2. After 72 h of culture, the medium in the well was replaced with the fresh medium containing plain GPs, RIF-GPs and RIF at the concentrations equivalent to 1 mg/mL of drug. After 12 h, 50 μL MTT solution (5 mg/mL in PBS) was added to each well, and incubated at 37 ± 1 °C for 4 h for MTT formazan formation. Subsequently the supernatant was carefully removed and formazan crystals were dissolved in DMSO. The plates were then mildly shaken for 10 min to ensure the dissolution of formazan. The absorbance values were measured by using microplate reader (Bio-Rad, Model 550-Microplate Reader, USA) at wavelength 570 nm, blanked with DMSO solution (Lee et al., 2006; Kumar et al., 2006; De Souza et al., 2004). Three replicates were read for each sample and mean value was used as the final result. The spectrophotometer was calibrated to zero absorbance using culture medium without cells. The relative cell viability (%) related to control wells containing cell culture medium without nanoparticles was calculated by Eq. (4):

$$\text{Cell viability (\%)} = \frac{[A]_{\text{test}}}{[A]_{\text{control}}} \times 100 \quad (4)$$

where $[A]_{\text{test}}$ is the absorbance of the test sample and $[A]_{\text{control}}$ is the absorbance of control sample.

2.3.7. In vivo drug distribution studies

The study was approved by the Animal Ethics Committee of Dr. H.S. Gour University Sagar (MP) India. Balb/C mice weighing 20–30 g were used for this study. The dose of RIF used was 10 mg kg^{-1} body weight of mice (Labana et al., 2002). Mice were divided into four groups each containing 24 animals and the following formulations were administered.

Group 1: GPs containing RIF given intravenously.
Group 2: Aqueous RIF solution orally (conventional dose).
Group 3: Empty nanoparticulate formulation given intravenously (a positive control group to exclude the influence of GPs on drug assay).
Group 4: Kept as control and given PBS (pH 7.4) to exclude the influence of PBS on drug assay.

Following the drug administration, animals from each groups were bled via the retro-orbital plexus at different time points, plasma was separated and analysed for the drug. In addition, the animals were sacrificed at various time points and the drug content analysed in 20% organ homogenates (i.e. 50 mg of the organs homogenized in 250 μL isotonic saline) of lungs, liver and spleen. The results are expressed as μg drug per mL plasma and percentage of drug distributed to organs after particular time intervals. The drug concentrations in plasma and organ homogenates were measured by HPLC method reported by Guillaumont et al. (1982). Briefly, the plasma and organ homogenates obtained from each mice were deproteinized with 100 μL of acetonitrile, vortexed for 5 min and centrifuged at 5000 × *g* for 20 min at 4–8 °C. The supernatant was used for the analysis of RIF upon suitable dilution with mobile phase [methanol:0.5 M ammonium formate (65:35) containing 5 mM heptane sulphuric acid and 1.5 mL of butanol:chloroform (30:70)]. The instrument (Shimadzu, Japan) comprising of a pump LC-10AT vp equipped with universal injector 7725i (rheodyne) with an injection volume of 20 μL, SPD-10A vp variable wavelength UV–vis detector (Shimadzu) and Shimadzu class-vp software version 5.03, A C-18 reverse phase column (Luma, particle size-5 μm, column size 250 mm × 4 mm) was used. The drug was analyzed by HPLC and compared with calibration graphs (obtained by analyzing pooled blank plasma and organ homogenates spiked with known drug amounts).

2.3.8. Pharmacokinetic analysis

The plasma drug profile was obtained and the data was used to determine various pharmacokinetic parameters. Peak plasma concentration (C_{max}) and time taken to reach C_{max}, (T_{max}) were computed from the curve. The area under the concentration–time curve (AUC_{0-t}) was determined by the trapezoidal rule. The terminal $AUC_{t-\infty}$ was obtained by dividing the last measurable plasma drug concentration by the elimination rate constant (obtained by regression analysis). The sum of AUC_{0-t} and $AUC_{t-\infty}$ yielded the total $AUC_{0-\infty}$ while the area under moment curve (AUMC)/area under curve (AUC) gave the mean residence time (MRT).

2.3.9. In vivo antitubercular activity

Mice (Balb/C) were infected with 1×10^5 colony forming units (CFU) of *M. tuberculosis* H37Rv through the aerosol route (Glascol-Inhalation Exposure System, USA). With this device, compressed

Table 1
Characterization of gelatin nanoparticles (mean ± S.D., $n = 3$).

Formulation code	Surface morphology	Particle size (nm)	PDI	Zeta potential (mV)	Entrapment efficiency (%)	Actual drug loading (w/w%)	Nanoparticles yield (w/w%)
Blank	Smooth	234 ± 14	0.13 ± 0.021	18.5 ± 0.25	–	–	68.3 ± 2.34
RIF loaded	Smooth	264 ± 11.2	0.24 ± 0.011	15.32 ± 0.19	59.5 ± 0.82	2.3 ± 0.14	63.7 ± 3.1

air is pumped into the chamber through a venturi nebulizer in which 10 mL of bacterial suspension at a concentration of 10^5/mL was placed. The nebulizer was drained for about 30 min and in this period the mice within the chamber inhaled approximately 50–100 bacilli into their bronchial tree and alveolar spaces. Twenty hours after infection, three mice from control group were sacrificed and lungs and spleen were homogenized with phosphate buffer and plated on Middlebrook 7H10 agar plates (Sigma, USA) to obtain the CFU of the infected animals after 21–28 days.

Mice were divided into various groups of six animals each. Group 1 served as control, Group 2 was given empty GPs suspended in PBS. Group 3 received a free RIF at doses of 10 mg/kg body weight orally daily for 4 weeks and Group 4 were given the same dose RIF encapsulated in GPs. Drugs were administered intravenously every three days for a period of four weeks except for oral group. The animals were sacrificed on day 30 following the initiation of chemotherapy. Fifty microliters of undiluted, 1:100 diluted and 1:1000 diluted aliquots of lung/spleen homogenates were inoculated on Middlebrook 7H10 agar base supplemented with oleic acid-albumin-dextrose-catalase (OADC) enrichment medium (Sigma, USA). Colony forming units (CFU) were enumerated after 3–4 weeks of inoculation and the data were analyzed by one-way analysis of variance (ANOVA) followed by unpaired Student's *t*-test to compare the untreated and treated groups.

2.3.10. Statistical analysis

Statistical analysis was performed with Graph Pad Instat Software (Version 3.00; Graph Pad Software, San Diego, CA, USA). Analysis of variance (ANOVA) was used to test the statistical significance of differences among groups. Statistical significance in the differences of the means was evaluated by using Student's *t*-test or Dunnett's test for the single or multiple comparisons of experimental groups, respectively. Difference with $P < 0.05$ was considered statistically significant.

3. Result and discussion

3.1. Preparation and characterization of gelatin nanoparticles

GPs prepared using modified two-step desolvation technique using acetone as desolvating agent and gluteraldehyde as a cross-linking agent have been found to be highly stable in water and cell medium. This method leads to the formation of least aggregated particles with uniform distribution. The sediment obtained after first desolvation step mainly possessed the high molecular weight gelatin while the supernatant, which was removed, was containing dissolved gelatin and low molecular weight portion of gelatin (Coester et al., 2000; Nahar et al., 2008). The purpose of removing low molecular weight gelatin was to avoid wider distribution of molecular weight of gelatin, which may not only cause formation of irreversible aggregates after cross-linking but may also form unstable particles.

The average particle size of GPs was found to be 264 ± 11.2 nm. A very low polydispersity index (PDI) of nanoparticles suggested the narrow size distribution of the nanoparticles. The results of entrapment efficiency, yield, practical drug loading, and zeta potential are summarized in Table 1. The TEM photomicrograph revealed that the GPs were spherical in shape (Fig. 1). The AFM is able to create

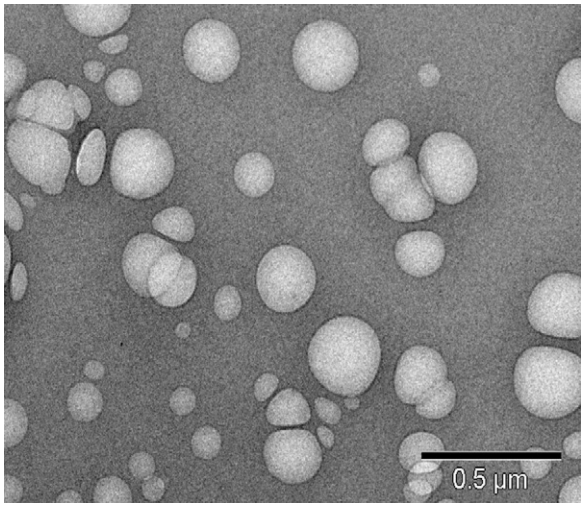

Fig. 1. TEM photomicrograph of gelatin nanoparticles.

three-dimensional photomicrographs with a resolution down to the nanometeric scales, which can be used as an important tool for cell biology. AFM photomicrograph also represented that GPs were having spherical shape and uniform size (Fig. 2). The zeta potential of drug loaded GPs was 15.32 ± 0.19 mV (Table 1), and this elevated value of zeta potential indicates high electric charge on the surface of the RIF-GPs, which is responsible for the strong repulsive forces amongst the particles that prevents their aggregation in buffer solution and favors formation of stabilized nanoparticles. The similar results were obtained by Nahar et al. (2008). The UV–vis spectra of RIF-loaded GPs and pure RIF were recorded. The RIF-loaded GPs spectrum showed a peak with a slight shift in λ_{max} from 476 to 474.6 in PBS pH 7.4 solution but with decreased intensities. This showed that the RIF is highly compatible with the gelatin in GPs.

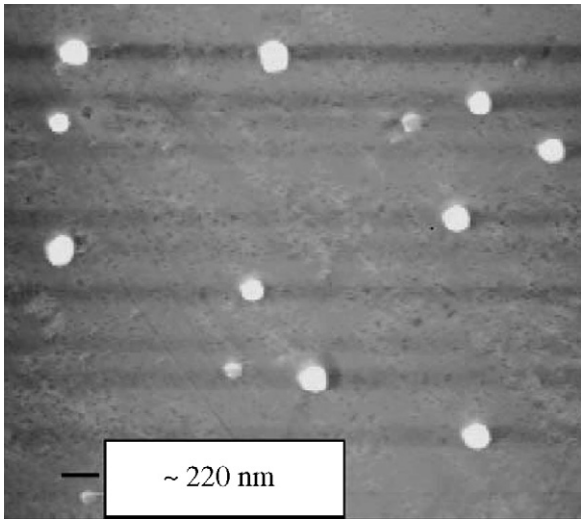

Fig. 2. AFM photomicrograph of gelatin nanoparticles.

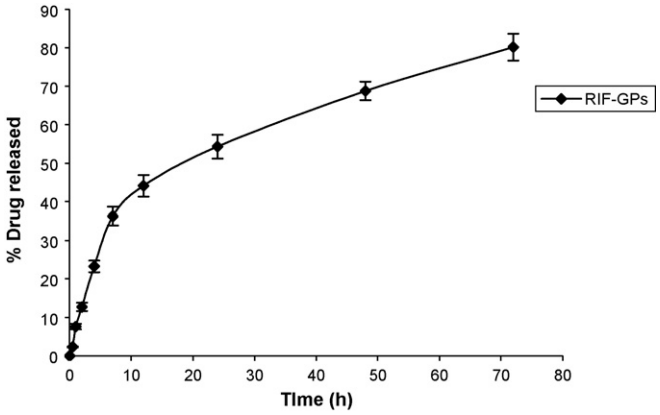

Fig. 3. *In vitro* drug release from rifampicin loaded nanoparticles (values represent mean ± S.D., $n = 3$).

3.2. In vitro drug release studies

The *in vitro* drug release of RIF-loaded GPs was studied for 72 h at pH 7.4 by using a dialysis membrane (Fig. 3). In the first 12 h 42% of RIF was released from the nanoparticles, which increased to 48% in 24 h followed by a gradual and sustained release up to 81.4% in 72 h. The release behavior of drug from the gelatin matrix showed a biphasic pattern that is characterized by an initial burst, followed by a sustained release. The initial-burst release may have occurred due to the release of drug present at or just beneath the surface of the nanoparticles. Then, release may have occurred due to the diffusion of drug molecules through the polymeric matrix of the nanoparticles. The biphasic release from the GPs was found to be similar to that previously reported by other research groups (Leo et al., 1999; Verma et al., 2005; Nahar et al., 2008).

3.3. Ex vivo cytotoxicity assay

The MTT assay is an established colorimetric method based on the determination of cell viability, utilizing the reaction of a tetrazolium salt with the mitochondria of metabolically active cells. The reduction of the tetrazolium salt by NADP (nicotinamide adenine dinucleotide phosphate) and NADPH (nicotinamide adenine dinucleotide hydrogen phosphate) within the cells produces insoluble purple formazan crystals, which are later solubilized yielding a purple-colored solution. The biocompatibility of GPs was tested using MTT assay on J774 cells. Cells incubated with GPs and RIF-GP remained nearly 100% viable when compared to the control group at concentrations as high as 1 mg/mL (Fig. 4). The cell viability was

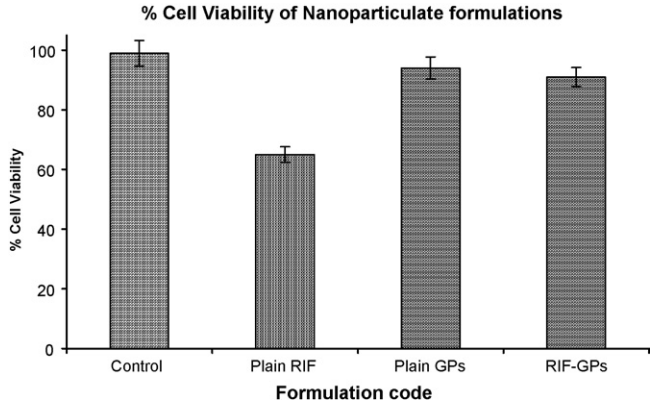

Fig. 4. Cell viability studies on J774 cells after 72 h exposure (values represent mean ± S.D., $n = 3$).

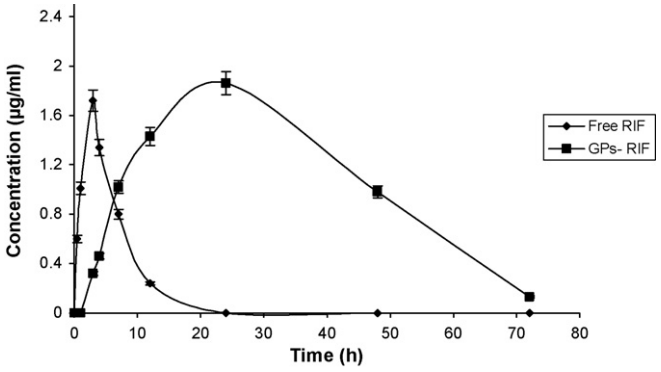

Fig. 5. Plasma drug profile of RIF and RIF-loaded GPs (values represent mean ± S.D., $n = 3$).

94%, 91% and 65%, respectively for GPs, RIF-GPs and RIF treated cells, at 1 mg/mL concentration. A significant evidence ($P \leq 0.05$) of lesser cytotoxicity was observed for GPs and RIF-GPs as compared to free RIF after 72 h of treatment. These results clearly indicated that GPs, even with a varied degree of modification were biocompatible and non-toxic to normal J774 cells. Similar results of MTT assay were reported by other research groups (De Souza et al., 2004; Lee et al., 2006).

3.4. In vivo drug distribution studies

The biodistribution studies clearly indicate superiority of the nanoparticulate RIF in contrast to the plain drug in increasing the accumulation of RIF within the organs rich in macrophages (liver, lungs and spleen). Following a single administration of RIF loaded GPs to mice the drug was detectable in the plasma from 3 h onwards up to 72 h. At each time point, the drug concentrations were at or above the minimum effective concentration required to kill the mycobacterium. On the other hand free drug solution was found to be cleared quickly from the blood (Fig. 5). However; the blood level from RIF-GPs was lower than plain drug that may possibly be due to relatively slower release of RIF from nanoparticles. The estimated amount of drug in liver, kidney, spleen and lung at different time intervals for 24 h after administration of free RIF revealed that maximum accumulation of the drug in these organs was achieved within 1–2 h of oral administration. The accumulation of drug in different macrophage rich organs (24.1 ± 1.2% in lungs, 33.1 ± 1.1% in liver and 10.7 ± 1.2% in spleen) from RIF-GPs was significantly higher ($P \leq 0.05$) as compared to free drug after 4 h interval. This can be accounted to be 6 fold enhancement in case of lungs, 2.5 fold in case of liver, and about 3.0 fold in case of spleen, respectively (Fig. 6). The C_{max} was comparable after oral administration of the RIF versus intravenous delivery of encapsulated drug (Table 2). The slow and

Table 2
Pharmacokinetics of RIF loaded in gelatin nanoparticles as compared to free drugs in mice.

Parameter	Rifampicin	
	Free	loaded
C_{max} (µg/mL)	1.72 ± 0.24	1.86 ± 0.19
T_{max} (h)	3.00 ± 0.00	24 ± 0.00
K_{el} (h^{-1})	0.217 ± 0.13	0.024 ± 0.2
$t_{1/2}$ (h)	3.2 ± 0.70	28.87 ± 3.22
MRT (h)	5.42 ± 1.00	33.64 ± 2.71
$AUC_{0-\infty}$ (µg h/mL)	7.36 ± 1.10	87.98 ± 3.63*

Values are mean ± S.D., $n = 3$. *$P \leq 0.001$ with respect to free drugs, according to Student's unpaired t-test. C_{max} = peak plasma concentration; T_{max} = time taken to reach C_{max}; K_{el} = elimination rate constant; $t_{1/2}$ = elimination half life; MRT = mean residence time; $AUC_{0-\infty}$ area under plasma drug concentration over time curve.

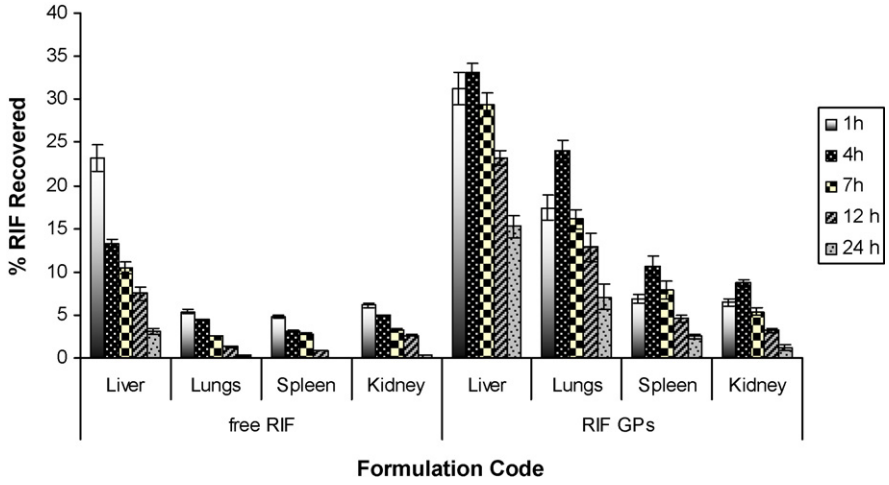

Fig. 6. *In vivo* organ distribution of RIF and RIF-loaded GPs (values represent mean ± S.D., $n = 3$).

Table 3
Chemotherapeutic efficacy of various formulations against experimental tuberculosis in mice.

Groups	$\log_{10}$ cfu	
	Lung	Spleen
Untreated controls	6.1 ± 0.31*	3.0 ± 0.42*
Empty gelatin nanoparticles	6.02 ± 0.52	3.1 ± 0.21
RIF solution everyday orally (30 doses)	4.5 ± 0.11*	2.2 ± 0.13*
RIF loaded gelatin nanoparticles every 3 days intravenously (10 doses)	3.4 ± 0.18*	1.76 ± 0.10*

Results are mean ± S.D. ($n = 6$); *$P \leq 0.05$ (Student's t-test), with respect to the untreated controls.

sustained release of RIF from GPs accounts for the long time (T_{max}) required for attaining C_{max}. The slow elimination rate (K_{el}) resulted in significantly prolonged $t_{1/2}$ of RIF compared to conventional oral administration of the drug. The area under curve (AUC) corresponds to the integral of the plasma concentration versus an interval of definite time, which was also found to be significantly higher ($P \leq 0.05$) as compared to the free drug (Table 2). Further, AUC and MRT values provide an evidence for the increased bioavailability of rifampicin in encapsulated form (GPs) as compared to free RIF. The above data justify the efficacy of the formulation as a sustained release system for temporal and spatial distribution of drug.

3.5. *In vivo* antitubercular activity

To assess the antimycobacterial activity of encapsulated versus free RIF *in vivo*, mice were infected via aerosolized route with 1×10^5 number of viable *M. tuberculosis*. After a 4-week treatment period, a significant reduction ($P \leq 0.05$) in the bacterial loads of lungs and spleen organs was observed for treated mice in contrast with untreated mice. The nanoparticulate drug depicted almost two fold reduction in CFU of mycobacteria in lungs and spleen when compared with untreated animals. Moreover, the administration of RIF loaded GPs resulted in a significant reduction ($P \leq 0.05$) in the number of bacilli recovered both from the lungs and spleen as compared with of free RIF given through conventional route (Table 3). Though similar results were obtained with other drugs and carrier systems (Pandey et al., 2003; Gaspar et al., 2008) as well as with ligand-appended synthetic polymer based nanoparticles (Sharma et al., 2004), the need for large amounts of the polymer, biodegradability, cost restriction of the polymer, the hazard of residual organic solvents and a lower drug stability are some of the critical factors that shift the choice of formulation towards biodegradable nanoparticles such as gelatin nanoparticles. Although in the present study, both conventionally administered and nanoparticulate drug were efficacious, yet it should be emphasized that 28 doses (oral RIF daily) have been reduced to ten doses (RIF-GPs administered iv every 3 days). The results encompass a crucial bearing since the reduction in dosing frequency would certainly enhance the patient compliance and hence, improve the management of TB.

4. Conclusion

In the last 25 years, polymeric drug delivery systems have been extensively utilized for various therapeutic and biomedical applications. Synthetic (e.g. polycaprolactone, polylactide-co-glycolide or PLG, etc.) as well as natural (e.g. gelatin, alginate, chitosan, etc.) polymers have potentials of encapsulating a wide range of bioactives of therapeutic interest. The gelatin nanoparticles were successfully prepared by two-step desolvation method encapsulating rifampicin. The prepared carrier system had particle size in nanometric range with lower polydispersity index suggesting the uniform distribution of the particles. The nanoparticulate system showed a controlled drug release upto 72 h suggesting a possible advantage of a sustained release formulation. The prepared system showed lower cytotoxicity and enhanced uptake of drug by the lung tissue, improving the AUC, MRT and hence bioavailability. Moreover, GPs showed improved chemotherapeutic efficacy of the drug as compared to conventional therapy. Hence, it may be concluded that GPs may be utilized as potential tool for the delivery of bioactives to the lung tissues leading to minimized side effects and improving the therapeutic efficacy of the drug.

Acknowledgements

Authors are grateful to M/s Lupin Ltd., Pune, India, for providing Rifampicin as a gift sample. Director, Electron Microscopy Section, AIIMS, New Delhi, India is acknowledged for providing the facilities for electron microscopy. The authors are also grateful to the Indian Council for Medical Research, New Delhi, India, for providing financial assistance to carry out this work.

References

Ahmad, Z., Pandey, R., Sharma, S., Khuller, G.K., 2008. Novel chemotherapy for tuberculosis: chemotherapeutic potential of econazole- and moxifloxacin-loaded PLG nanoparticles. Int. J. Antimicrob. Agents 31, 142–146.

Bajpai, A.K., Choubey, J., 2006. Design of gelatin nanoparticles as swelling controlled delivery system for chloroquine phosphate. J. Mater. Sci. Mater. Med. 17, 345–358.
Bala, I., Hariharan, S., Kumar, M.N., 2004. PLGA nanoparticles in drug delivery: the state of the art. Crit. Rev. Ther. Drug Carrier Syst. 21, 387–422.
Balthasar, S., Michaelis, K., Dinauer, N., von-Briesen, H., Kreuter, J., Langer, K., 2005. Preparation and characterization of antibody modified gelatin nanoparticles as drug carrier system for uptake in lymphocytes. Biomaterials 26, 2723–2732.
Barrow, E.W., Winchester, G.A., Staas, J.K., Quenelle, D.C., Barrow, W.W., 1998. Use of microsphere technology for targeted delivery of rifampin to *Mycobacterium tuberculosis*-infected macrophages. Antimicrob. Agents Chemother. 42, 2682–2689.
Cascone, M.G., Lazzeri, L., Carmignani, C., Zhu, Z., 2002. Gelatin nanoparticles produced by a simple W/O emulsion as delivery system for methotrexate. J. Mater. Sci. Mater. Med. 13, 523–526.
Coester, C.J., Langer, K., Van-Briesen, H., Kreuter, J., 2000. Gelatin nanoparticles by two-step desolvation—a new preparation method, surface modifications and cell uptake. J. Microencapsul. 17, 187–193.
De Souza, A.O., Santos-Jr, R.R., Sato, D.N., de Azevedo, M.M.M., Ferreira, D.A., Melo, P.S., Celio, M.H., Silva, L., Duranc, N., 2004. Free 2-propen-1-amine derivative and inclusion complexes with β-cyclodextrin: scanning electron microscopy, dissolution, cytotoxicity and antimycobacterial activity. J. Braz. Chem. Soc. 15, 682–689.
Deol, P., Khuller, G.K., 1997. Lung specific stealth liposomes: stability, biodistribution and toxicity of liposomal antitubercular drugs in mice. Biochim. Biophys. Acta 1334, 161–172.
Gallo, G.G., Radaelli, P., 2005. Rifampicin. In: Florey, K. (Ed.), Analytical Profiles of Drug Substances. Vol. 5. Indian Reprints. Rajkamal Electric Press, New Delhi, pp. 469–513.
Gaspar, M.M., Cruz, A., Penha, A.F., Reymao, J., Sousa, A.C., Eleuterio, C.V., Domingues, S.A., Fraga, A.G., Longatto Filho, A., Cruz, M.E.M., Pedrosa, J., 2008. Rifabutin encapsulated in liposomes exhibits increased therapeutic activity in a model of disseminated tuberculosis. Int. J. Antimicrob. Agents 31, 37–45.
Gelperina, S., Kisich, K., Iseman, M.D., Heifets, L., 2005. The potential advantages of nanoparticle drug delivery systems in chemotherapy of tuberculosis. Am. J. Resp. Crit. Care Med. 172, 1487–1490.
Guillaumont, M., Leclercq, M., Frobert, Y., Guise, B.J., 1982. Determination of rifampicin, desacetylrifampicin, isoniazid and acetylisoniazid by high-performance liquid chromatography: application to human serum extracts, polymorphonucleocytes and alveolar macrophages. Chromatogr. B: Biomed. Appl. 232, 369–376.
Gupta, U.D., Katoch, V.M., 2009. Animal models of tuberculosis for vaccine development. Indian J. Med. Res. 129, 11–18.
Jain, S.K., Gupta, Y., Jain, A., Saxena, A.R., Khare, P., Jain, A., 2008. Mannosylated gelatin nanoparticles bearing an anti-HIV drug didanosine for site-specific delivery. Nanomed.: Nanotechnol. Biol. Med. 4, 41–48.
Kaul, G., Amiji, M., 2005. Tumor-targeted gene delivery using poly(ethylene glycol)-modified gelatin nanoparticles: in vitro and in vivo studies. Pharm. Res. 22, 951–961.
Kaur, A., Jain, S., Tiwary, A.K., 2008. Mannan-coated gelatin nanoparticles for sustained and targeted delivery of didanosine: *in vitro* and *in vivo* evaluation. Acta Pharm. 58, 61–74.
Kisich, K.O., Gelperina, S., Higgins, M.P., Wilson, S., Shipulo, E., Oganesyan, E., Heifets, L., 2007. Encapsulation of moxifloxacin within poly(butyl cyanoacrylate) nanoparticles enhances efficacy against intracellular *Mycobacterium tuberculosis*. Int. J. Pharm. 345, 154–162.
Kreuter, J., 2004. Nanoparticles as drug delivery system. In: Nalwa, H.S. (Ed.), Encyclopedia of Nanoscience and Nanotechnology, vol. 7. American Scientific Publishers, New York, USA, pp. 161–180.
Kumar, P.V., Asthana, A., Dutta, T., Jain, N.K., 2006. Intracellular macrophage uptake of rifampicin loaded mannosylated dendrimers. J. Drug Target. 14, 546–556.
Labana, S., Pandey, R., Sharma, S., Khuller, G.K., 2002. Chemotherapeutic activity against murine tuberculosis of once weekly administered drugs (isoniazid and rifampicin) encapsulated in liposomes. Int. J. Antimicrob. Agents 20, 301–304.
Laura, J.V.P., Kerstin, J.W., Vito, R., 2000. Accumulation of rifampicin by *Mycobacterium aurum*, *Mycobacterium smegmatis* and *Mycobacterium tuberculosis*. J. Antimicrob. Chemother. 45, 159–165.
Lee, G.Y., Park, K., Nam, J.H., Kim, S.Y., Byun, Y., 2006. Anti-tumor and anti-metastatic effects of gelatin-doxorubicin and PEGylated gelatin-doxorubicin nanoparticles in SCC7 bearing mice. J. Drug Target. 14, 707–716.
Leo, E., Vandelli, M.A., Cameroni, R., Forni, F., 1997. Doxorubicin-loaded gelatin nanoparticles stabilized by glutaraldehyde: involvement of the drug in the cross-linking process. Int. J. Pharm. 12, 75–82.
Leo, E., Cameroni, R., Forni, F., 1999. Dynamic dialysis for the drug release evaluation from doxorubicin-gelatin nanoparticles conjugates. Int. J. Pharm. 180, 23–30.
Li, J.K., Wang, N., Wu, X.S., 1998. Gelatin nanoencapsulation of protein/peptide drugs using an emulsifier-free emulsion method. J. Microencapsul. 15, 163–172.
Nahar, M., Mishra, D., Dubey, V., Jain, N.K., 2008. Development, characterization, and toxicity evaluation of amphotericin B-loaded gelatin nanoparticles. Nanomed. Nanotech. Biol. Med. 4, 252–261.
Pandey, R., Khuller, G.K., 2005. Solid lipid particle-based inhalable sustained drug delivery system against experimental tuberculosis. Tuberculosis (Edinb) 85, 227–234.
Pandey, R., Khuller, G.K., 2007. Nanoparticle-based oral drug delivery system for injectable-antibiotics streptomycin. Chemotherapy 53, 437–441.
Pandey, R., Sharma, A., Zahoor, A., Sharma, S., Khuller, G.K., Prasad, B., 2003. Poly (DL-lactide-coglycolide) nanoparticle-based inhalable sustained drug delivery system for experimental tuberculosis. J. Antimicrob. Chemother. 52, 981–986.
Sharma, A., Sharma, S., Khuller, G.K., 2004. Lectin functionalised poly(lactide-co-glycolide) nanoparticles as oral/aerosolized antitubercular drug carriers for treatment of tuberculosis. J. Antimicrob. Chemother. 54, 761–766.
Soppimath, K.S., Aminabhavi, T.M., Kulkarni, A.R., Rudzinski, W.E., 2001. Biodegradable polymeric nanoparticles as drug delivery devices. J. Control. Release 70, 1–20.
Toit, L.C., Pillay, V., Danckwerts, M.P., 2006. Tuberculosis chemotherapy: current drug delivery approaches. Resp. Res. 7, 1–18.
Truong-Le, V.L., Walsh, S.M., Schweibert, E., Mao, H.Q., Guggino, W.B., August, J.T., et al., 1999. Gene transfer by DNA-gelatin nanospheres. Arch. Biochem. Biophys. 361, 47–56.
Vandervoort, J., Ludwig, A., 2004. Preparation and evaluation of drug-loaded gelatin nanoparticles for topical ophthalmic use. Eur. J. Pharm. Biopharm. 57, 251–261.
Verma, A.K., Sachin, K., Saxena, A., Bohidar, H.B., 2005. Release kinetics from bio-polymeric nanoparticles encapsulating protein synthesis inhibitor—cycloheximide, for possible therapeutic applications. Curr. Pharm. Biotechnol. 6, 121–130.
World Health Organization, 2006. Global Tuberculosis Control: Surveillance, planning, financing WHO Report 2006.WHO/HTM/TB/2006.362 World Health Organization (WHO), Geneva. Available at http://www.who.int/tb/publications/global_ report/2006/en/.
Yeh, T.K., Lu, Z., Wientjes, M.G., Au, J.L.S., 2005. Formulating paclitaxel in nanoparticles alters its disposition. Pharm. Res. 22, 867–874.